HiSST: 3rd International Conference on High-Speed Vehicle Science Technology
14-19 April 2024, Busan, Korea

Numerical Study of Hydrogen Injection to initiate Oblique Detonation Wave

Ashish Vashishtha[1], Rushikesh Kore[2], Sasi Kiran Palateerdham[3], and Antonella Ingenito[4]

Abstract

With the motivation of operating scramjet in shock induced combustion ramjet (shcramjet) or oblique detonation wave mode, the current study aims to develop strategies for non-premixed oblique detonation wave configuration using numerical simulations. The unsteady two-dimensional Reynolds Averaged Navier-Stokes with reactive multi-species equations are solved using adaptive grid refinement and robust SAGE solver on CONVERGE-CFD platform with detailed chemical kinetics. The sonic hydrogen injection cases ($\phi = 0.5$) into incoming air flow at Mach 7 with pressure of 40 kPa and temperature of 300 K are simulated for 2 ms duration. The computational domain consists of finite length wedge (100 mm, $\theta_w = 26^\circ$ as well as hydrogen injection tube upstream of wedge starting point, to obtain non-premixed oblique detonation wave. The unsteady detonation wave patterns are obtained for angle of injection (AOI) 15° with injector location at (D_j=) 30 mm from wedge tip. It is found that various flow features, such as jet-shock, shear layer and hot burnt zone near the wedge wall affect the lifted detonation wave starting at the interaction point of shear layer and hot burnt zone. The detonation wave momentarily transition to deflagration flame and re-establish itself as detonation wave multiple times. The angle of injection (AOI) and injector locations are varied to obtain various patterns of unsteady non-premixed oblique detonation wave and it was found that AOIs below or close to wedge angle lead to formation of unsteady oblique detonation wave, while AOIs higher than the wedge angle lead to formation of stable stretched deflagration flame. Injection location very close to wedge starting point leads to multi-cycle detonation to deflagration transitions and deflagration to detonation transitions. The overall thermal and combustion efficiencies are also compared with equivalent premixed hydrogen-air oblique detonation wave at same wedge angle.

Keywords: *Numerical Simulations, Jet Injection, Shock induced Combustion, Detonation, Non-premixed combustion*

Nomenclature

Latin

P – Pressure
V – Velocity
M – Mach Number
T – Temperature
y – Mass Fraction
AOI – Angle of Injection
J – Momentum Flux Ratio = $\frac{\rho_j {V_j}^2}{\rho_\infty {V_\infty}^2}$

Greek

ρ – Density
θ – Angle of Wedge
β – OSW or ODW angle

Subscripts

∞ – Freestream
j – Jet
w – Wedge
CJ – Chapmann-Jouguet Condition
OSW – Oblique Shock Wave
ODW – Oblique Detonation Wave
H_2, OH, H_2O – Chemical Species

[1]*Lecturer, Department of Aerospace & Mechanical Engineering, South East Technological University, Carlow Campus, R93 V960, Ireland, ashish.vashishtha@setu.ie*
[2]*Postgraduate Student, Department of Aerospace & Mechanical Engineering, South East Technological University, Carlow Campus, R93 V960, Ireland*
[3]*PhD student, Scuola di Ingegneria Aerospaziale, Sapienza University of Rome, 00138, Italy*
[4]*Professor (Associate), Scuola di Ingegneria Aerospaziale, Sapienza University of Rome, 00138, Italy, antonella.ingenito@uniroma1.it*

1. Introduction

Shockwaves can be defined as a compression wave-front upstream of an object flying at the local speed more than the speed of sound. Shockwaves can affect flow properties across it, especially jump in pressure and temperature. The rise in temperature across the shock can be utilized for igniting fuel-air mixture in air-breathing hypersonic propulsion applications. Further, the shock induced ignited fuel-air mixture may turn from deflagration mode to detonation mode combustion in highly compressed zones and produce detonation wave at appropriate local flow conditions and fuel air mixture composition. Detonation wave differs than deflagration wave as it travels at supersonic speed with flame coupled with shockwave and the reaction products behind it. The pressure and temperature can have higher jump across the detonation wave [1]. In case of the deflagration wave, the flame can only travel at subsonic speeds and pressure remains almost constant across, while temperature increases across flame. There are few hypersonic propulsion concepts [2] based on detonation combustion (or pressure gain combustion), which have been extensively studied by many researchers in past decades: pulse detonation engine (PDE), rotatory detonation engine (RDE) and oblique detonation wave engine (ODWE or shock induced combustion ramjet, shcramjet). The advantages of detonation-based propulsion systems are: it can provide higher rate of energy release, higher thermodynamic efficiency as well as shorter combustion chamber in comparison to conventional deflagration combustion based systems. Among above three, pulse detonation engine has been initially studied extensively and it was found to have operational constraints because of the requirements of: long tubes for detonation transition, ignition source in each cycle and purging of combustion products in each cycle, which leads to lower frequency (few hundreds of Hz) operation. The rotary detonation engine (RDE) has annular cylindrical domain, which is advantageous than the PDE as it requires ignition only once and can operate at higher frequencies of the order of 1000s Hz. In RDE (both premixed/non-premixed) the fuel-air mixture is ignited once and the detonation wave travels in circumferential manner until all the fuel-air mixture is burnt. The Oblique detonation wave engine has simplest design, and it can be easily integrated in scramjet engine configuration. It requires a wedge in supersonic premixed stream of fuel-air mixture, which can establish a compression wave as oblique shock wave. Sufficient strength of oblique shock (can be controlled by wedge angle) can ignite fuel-air mixture and may turn it in standing or propagating detonation wave, which can be further accelerated through the nozzle. However, understanding of shock induced combustion and transition to oblique detonation waves, required detailed understanding of affecting operating parameters along with efficient fuel-air mixing strategies. Initial designs and study of operations of the above pressure gain combustion systems are mainly based on premixed fuel-air mixture, a physical ignition source such as spark plug, pre-detonator or shock induced combustion can be very much effective in premixed systems. There have been recent interest in non-premixed (mixing controlled) detonation based propulsion systems to provide controlled and long duration operations.

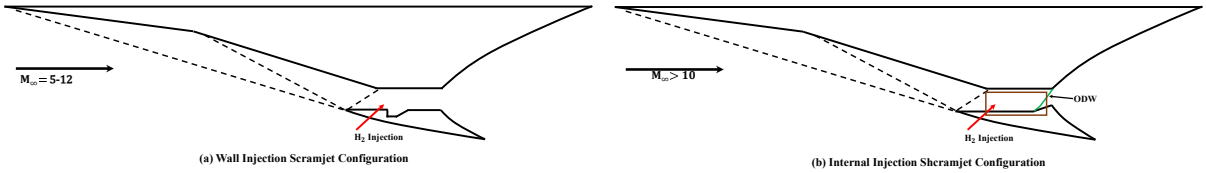

Fig 1. (a) Scramjet Configuration with wall fuel injection, (b) Internal Injection Shcramjet configuration

The current study is motivated to develop strategies for integrated system to operate as scramjet (supersonic deflagration combustion) and shcramjet (oblique detonation combustion) mode with non-premixed fuel injection. The scramjet configurations has been studied with various fuel injection methods such as angled wall-injection, wedge (compression/expansion ramp) based injection, pylon based injection and strut based injections [3, 4]. Figure 1a shows a typical scramjet configurations with wall injection, which required ignition method as well as cavity based flame holding method to establish the stabilized flame. In order to use the scramjet configuration with wall injection at higher freestream Mach numbers in oblique detonation mode, it will require fuel injection ahead of a wedge in combustor, which can provide sufficient compression to fuel-air mixture to ignite and turn into detonation flame as shown in

Fig. 1b. This configuration is called internal injection for Shcramjet Engine [5, 6]. Few recent studies conducted for external fuel injection for Shcramjet configuration, where the fuel is injected at the first two compression ramp [7, 8] to provide sufficient time for fuel-air to mix and develop premixed mixture before reaching the wedge to generate premixed oblique detonation wave. The current study uses numerical simulations with aim to develop understanding of fuel jet ignition by direct injection in cross-flow of hypersonic freestream ahead to wedge for the application of non-premixed oblique detonation wave engine. The main objectives of the current study can be described as: 1) Develop understanding of fuel-air injection in hypersonic cross-flow and its effect on establishing oblique detonation wave on a finite length wedge 2) comparatively quantify the effect of injection angle and injection location on establishing oblique detonation wave.

2. Numerical Method

The two-dimensional reactive multi-species Euler equations with detailed chemistry has been used to study various transition mechanism (smooth/abrupt) of oblique shock wave to oblique detonation wave and their dependency on freestream conditions for various fuel-air premixed mixtures [9–11]. In premixed mixture, the formation of stable oblique detonation wave on finite length wedge mainly depends on gas dynamic effects and chemical heat release rate, which can be modelled efficiently using adaptive grid refinement with high resolution (up to 16-64 grid points) within the half reaction zone. In premixed ODWE, it is conceptualized to inject fuel well before combustor (near the start of compression corner) to provide sufficient time to reach homogeneously well mixed fuel - air mixture in the combustor, which leads to longer length of overall system and may also cause pre-ignition. However, for more practical approach, it is required to inject fuel into high-speed flow region near the start of combustion chamber, before the finite length wedge. The sufficient compression provided by wedge and efficient mixing provided by injection method can lead to ignition of fuel-air mixture and may lead to formation of oblique detonation wave in non-premixed mode. Along with the gas dynamics, and chemistry modelling, the modelling of mixing phenomenon is important for such a case, which requires high-resolution of grid as well as turbulence modelling. Vashishtha et al. [12] and Harmon et al. [13] has modelled direct gas (H_2) injection into the stagnation zone of bow-shock in front of blunt nose and observed steady deflagration flame in short penetration mode as well as unsteady momentarily detonation in long penetration mode by performing two-dimensional simulation using various solvers. Recently, CONVERGE-CFD has been used to simulate complex rotating detonation phenomena by using its efficient adaptive grid resolution, incorporating turbulence modelling as well efficient chemistry solver SAGE which utilize adaptive zoning [14, 15]. Kore et al. [16] has utilized Converge-CFD for simulating the oblique detonation wave formation in premixed fuel-air mixtures along with different blends of hydrogen and methane. As the current study focuses on non-premixed oblique detonation wave modelling, it employs Converge-CFD for all the simulations to efficiently model fuel-air mixing, gas dynamics and chemical effects along with detailed chemistry.

2.1. Computational Domain and Modelling

Figure 2a shows the two-dimensional computational domain of 170 mm $\times$ 100 mm size with wedge at angle $\theta_w = 26°$. The fuel is injected at the bottom wall with 2 mm width tube at different injection (angle AOI) and injection distances (D_j) from the wedge starting point. The wedge tip started at X $= 0.0$ and at Y $= 0.0$, while two parameters Angle of Injection and Injection distance (D_j) are varied to establish shock induced detonation wave. The left side of domain is considered as Inlet and right side is considered as outlet, while topside is modelled as far-field with outlet boundary conditions.

The unsteady Reynolds Averaged Navier-Stokes equations of mass, momentum, species transport and total energy are solved with realizable k $- \varepsilon$ turbulence model in two-dimensional domain. Gas properties are calculated using an ideal gas equation. The second order spatial discretization with step flux limiter and fully implicit first-order accurate time integration method were used with PISO solver scheme. Variable time-stepping method with minimum time-step of 0.1 ns was employed, which was automatically calculated based on maximum CFL assigned. The simulations are stopped at 2 ms for all the cases. The solver uses cut-cell method and generate grid while simulations as well as uses adaptive mesh refinement (AMR) based on computed parameters. The simulation was initialized with only air in domain. The base grid of 4 mm is used during initialization, which was changed to 2 mm after 0.12 ms.

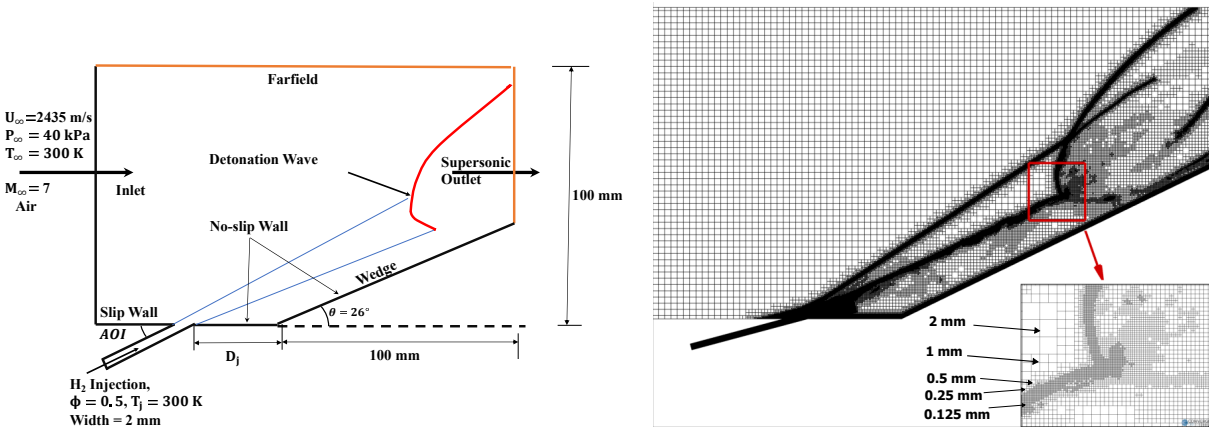

(a) Computational Domain **(b) Adaptive Grid Refinemen**

Fig 2. (a) Computational Domain, (b) Adaptive Grid Refinement for Mach 7, AOI 15° with $D_j = 30$ mm

Once the oblique shock was stabilized on the wedge with 2 mm base grid, the hydrogen injection as well as combustion was initiated at 0.15 ms. The adaptive grid refinement was controlled with parameters: velocity, temperature and for gas dynamics effects and with mass fraction of H_2, OH, O for mixing and flame front capturing up to level 4 (with minimum grid size of 0.125 mm). The sample grid with adaptive mesh refinement is shown in Fig. 2b for angle of injection 15° with injection location at $D_j = 30$ mm. The chemistry is modelled using Westbrook Mechanism [17] for H_2-Air combustion (with 12 species and 46 reactions), assuming Nitrogen as inert gas.

2.2. Boundary and Initial Conditions

The non-premixed oblique detonation wave configurations has been simulated for incoming air Mach number $M_\infty = 7$ with freestream pressure of 40 kPa and freestream temperature as 300 K. The incoming air and fuel injection inlet conditions are highlighted in Table 1. Hydrogen as fuel has been injected with 2 mm wide sonic injection tube at different angles and at different distances from the wedge tip. The pressure inlet with stagnation pressure and stagnation temperature are defined for inlet fuel boundary considering operating equivalence ratio (ϕ) of 0.5, which represents the momentum flux ratio (J) of 0.4. The right side and top boundaries in computational domain are considered supersonic outlet. The effect of angle of injection for a constant injection location and various injection locations for a single injector angle are simulated. The Angle of Injection (AOI) varied from shallow angle 10° to 90° for injection location 30 mm, while the injection locations are varied between 10 mm to 70 mm for AOI = 15°. The scramjet configuration requires a cavity to stabilize the flame [18], while oblique detonation wave requires a wedge to establish shock induced detonation wave. The finite length wedge of 100 mm and straight wall between starting point of wedge and injector are defined as no-slip adiabatic wall, while the injector walls and wall between injector and inlet boundary are defined as slip wall with zero normal gradient in temperature.

All the non-premixed simulations are performed for freestream incoming velocity of 2435.4 m/s with freestream pressure of 40 kPa and temperature of 300 K. To compare the efficiency of non-premixed oblique detonation wave configuration, an comparable premixed case has also been simulated at freestream incoming Mach number 7.0 for H_2- air equivalence ratio (ϕ = 0.5) at freestream pressure of 40 kPa and freestream temperature of 300 K as highlighted in Table 1. For given pressure (40 kPa), temperature (300 K) and equivalence ratio (ϕ = 0.5), the Chapmann-Jouguet speed (CJ-Speed) of detonation wave is 1619.1 m/s. The theoretical oblique detonation wave angle, calculated based on equilibrium condition is $\beta_{ODW} = 44.62°$ and theoretical pressure after oblique detonation wave is $P_{ODW} = 931.5$ kPa.

2.3. Grid Independence Study

The three grid configuration based on base grid of 2 mm (fine), 4 mm (medium) and 8 mm (coarse) are simulated for non-premixed oblique detonation wave configuration, while keeping the refinement

Table 1. Flow Conditions

Non-premixed Cases $\phi = 0.5$		
Property	**Inlet Air**	**Inlet Fuel**
Mach Number	M_∞ = 7.0	M_j = 1.0
Pressure	P_∞ = 40 kPa	P_j = 777 kPa
Temperature	T_∞ = 300 K	T_j = 300 K
Velocity	V_∞ = 2435.4 m/s	V_j = 1316.4 m/s
H_2 Mass Fraction	0	1
O_2 Mass Fraction	0.233	0
N_2 Mass Fraction	0.767	0
Momentum Flux Ratio (J)	-	0.4
Angle of Injection (AOI) for D_j = 30 mm	-	10°, 15°, 30°, 45°, 90°
Injector Location (D_j) for AOI = 15°	-	10, 30, 50, 70 mm
Premixed Case, $\phi = 0.5$	**Air-Fuel Mixture**	
Mach	M_∞ = 7.0	
Pressure	P_∞ = 40 kPa	
Temperature	T_∞ = 300 K	
Velocity	V_∞ = 2659.5 m/s	
H_2-Air Equivalence Ratio	0.5	
C-J Speed	V_{CJ} = 1619.1 m/s	
C-J Pressure	P_{CJ} = 470.5 kPa	
ODW Equilibrium Angle	$\beta_{ODW} = 44.62°$	
ODW Equilibrium Pressure	$P_{ODW} = 931.5$ kPa	

and adaptive mesh refinement strategies same for all the three cases. During 2 ms of total simulation, the grid is refined with level 1 for all cases at 0.12 ms before H_2 injection and starting of combustion at 0.15 ms. Further 4 levels of refinements are used with adaptive grid refinement based on velocity, temperature, mass fractions of H_2, O and OH. For all three cases, the overall thermal efficiency is calculated based on integrated heat release for the duration of simulation time and overall combustion efficiency is calculated based on remaining H_2 mass at the end of 2 ms simulation using following relations:

$$\eta_{th} = \frac{\int_0^t HRR dt}{LHV_{H_2} \times \int_0^t \dot{m}_{H_2,injected} dt} \qquad \eta_c = 1 - \frac{m_{H_2,unburnt}}{\int_0^t \dot{m}_{H_2,injected} dt} \tag{1}$$

Table 2. Grid Idependence Study

Grid Configuration	**Minimum Grid Size**	**Cell Count**	η_{th}	η_c
Coarse (Base = 8 mm)	0.25 mm	30921	0.549	0.926
Medium (Base = 4 mm)	0.125 mm	81974	0.520	0.928
Fine (Base = 2 mm)	0.0625 mm	195068	0.521	0.925

The overall results are compared in Table 2. With all three grid conditions, the overall combustion efficiency doesn't vary more than 1 %, while the thermal efficiency based on integrated heat release rate remains within 1 % between medium and fine grid case. The medium grid is selected in current

study based on available computing resources. In order to capture cellular structure and triple point of detonation wave, it will be required to refine grid further down to 3-4 more levels (of the order of 7-15 μm) [11], however the current selection of grid is sufficient to the defined objectives of study to understand the effect of geometrical parameters on oblique detonation wave initiation in non-premixed mode.

3. Results & Discussions

The mixing controlled oblique detonation wave in non-premixed mode of transverse wall injection is affected by efficiency of fuel-air mixing within the vicinity of wedge and fuel injector. The well mixed fuel-air mixture can ignite itself due to compression provided by the finite length wedge at certain angle. The fuel injection angle as jet in hypersonic cross-flow will also have significant impact to initialize oblique detonation wave as the distribution of fuel into the incoming hypersonic air cross-flow in the vicinity of wedge is effected by generation of bow-shock in front of injection point. Additionally, it is understood that high angle of injection can lead to stronger bow-shock in front of injection location may lead to early ignition near the fuel-jet injection location, which causes lesser availability of fuel-air mixture at downstream location of wedge. It requires a balance between fuel-air mixing, avoiding early ignition near the injection point and providing sufficient compression by finite length wedge to initiate oblique detonation wave in non-premixed mode. In order to understand the impact of injection angle and gap between injector and wedge starting point, total 8 cases are simulated by varying angle of injection (AOI) (5 cases), while keeping injector location as 30 mm from wedge starting point and by varying injector location (3 additional cases), while keeping injection angle as 15° in this study. Additionally, a premixed case with same incoming Mach number and equivalence ratio of fuel-air mixture (assuming perfect mixing) is also simulated. The mixing controlled non-premixed oblique detonation wave is essentially an unsteady phenomenon in comparison to premixed case (once the oblique detonation wave is established for stable $\theta - \beta -$ M combination). There are many pattern observed in the non-premixed simulations, while the detonation wave can travel back and forth along the wedge and momentarily can convert to deflagration mode with induced ignition within the shear layer between jet shock and starting of wedge. The results are discussed in term of overall efficiencies computed by thermal and combustion efficiencies according to Eq. 1 as well as detonation and deflagration pattern observed in various simulation cases along with premixed case.

3.1. Premixed Oblique Detonation

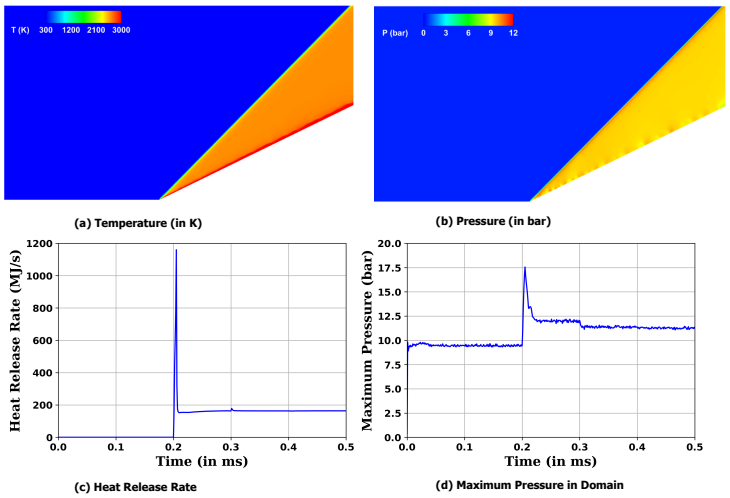

Fig 3. Premixed H_2-Air ($\phi = 0.5$) Case: (a) Temperature, (b) Pressure, (c) Heat Release Rate with time, (d) Maximum Pressure with time

Initially, premixed oblique detonation wave configuration has been simulated for incoming homogeneously mixed fuel-air mixture ($\phi = 0.5$) at Mach 7 and freestream pressure of 40 kPa and temperature of 300 K. As the Chapmann-Jouguet speed of detonation wave for given mixture is 1619.1 m/s, the

incoming flow speed is 1.64 times of the CJ-Speed, the oblique shock to oblique detonation wave transition occur in smooth manner almost near the wedge tip as seen in temperature and pressure plot of Fig. 3a & b. The oblique detonation wave forms angle of 45° similar to theoretical detonation wave angle of 44.62° for the wedge of 26° at Mach 7. The simulation is started without combustion initially, once the oblique shock wave is established, the combustion is started at 0.2 ms, which reflects in peak heat release rate in Fig. 3c and peak maximum pressure in Fig. 3d. The premixed oblique detonation wave shows stable flow field, hence the simulation is stopped at 0.5 ms in this case. The pressure behind oblique detonation wave is predicted as 10.4 bar, which is also close to theoretical pressure 9.31 bar as predicted with equilibrium conditions. The combustion efficiency for premixed configuration is computed closed to 1.0, while thermal efficiency based on integrated heat release rate is 0.95.

3.2. Non-Premixed Oblique Detonation

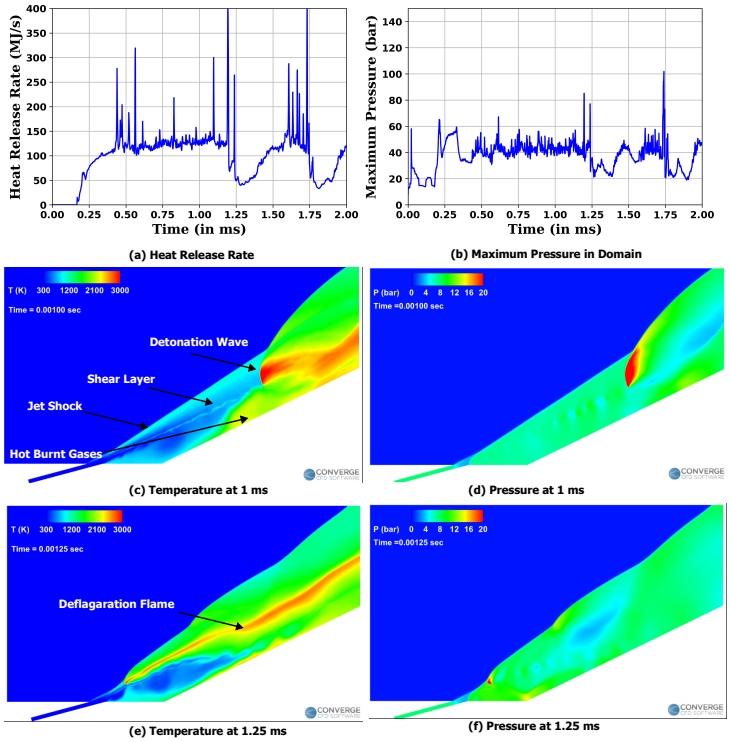

Fig 4. Non-premixed Detonation Case (AOI = 15° & $D_j = 30$ mm: (a) Heat Release Rate, (b) Maximum Pressure with time, (c,d) Temperature & Pressure in Detonation Mode, (e,f) Temperature & Pressure in Deflagration Mode

In this section, the dynamics of non-premixed oblique detonation wave configuration for angle of injection 15° and injector location $D_j = 30$ mm is analyzed with different flow patterns observed during the 2 ms simulation. Figure 4 a and b shows the heat release rate and maximum pressure in the domain for the duration of 2 ms. In the simulation, hydrogen is injected at 0.15 ms as well as combustion is initiated after the oblique shock wave is established at the wedge. Initially, hydrogen penetrate through the boundary layer on the wedge and interact with oblique shock wave. With achieving sufficient mixing with air and compression provided by the wedge, the flame is initiated in the boundary layer and detonation occur at axial distance of 0.016 m of the wedge. The sudden peaks in heat release rate curve are observed up to 1.25 ms, which is due to multi-detonation fronts interacting. The heat release rate remains close to constant up to 1.25 ms, which reflects the existence of detonation wave during this time period. The detonation wave travels along the wedge and establish itself by lifting away from the wall as shown in Fig 4 c and d. The flow pattern in Fig 4c and d shows lifted detonation wave where shock and flame are combined together. The detonation wave is fed by shear layer and hot burnt gases attached to wedge wall. As the mixing of fuel-air mixture is controlled by shear layer between

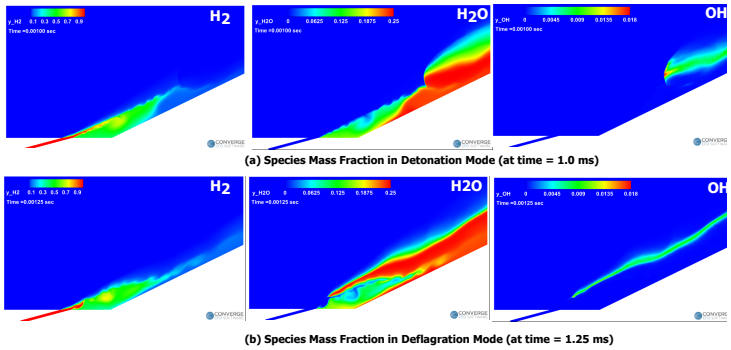

Fig 5. Non-premixed Detonation Case (AOI = 15° & $D_j = 30$ mm: (a) Species Mass Fraction in Detonation Mode, (b) Species Mass Fraction in Deflagration Mode

jet shock and wedge wall, the flow remains unsteady and detonation wave travels back and forth on the wedge with additional detonation front generated near interaction point of hot burnt gases and shear layer. At time 1.25 ms, there is sudden drop in heat release rate, which corresponds to ignition of fuel-air mixture in between shear layer and jet oblique shock, which turns the detonation wave into deflagration wave. The temperature and pressure contours for deflagration mode are shown in Fig. 4 e and f. The deflagration flame detaches from the shockwave, stretches along the wedge. Within 0.05 ms, the deflagration flame turns into detonation and starts establishing itself on the wedge. However after time 1.75 ms, there is another ignition between shear layer and jet shock turns detonation wave into deflagration flame and continues to form detonation wave by the end of simulation time.

Fig. 5 shows the species mass fraction of H_2,H_2O and OH for angle of injection 15° and injector location $D_j = 30$ mm in detonation as well as deflagration mode. In detonation mode, the H_2 mass is lifted towards the shear layer before the flame due to hot burnt gas region, which can be source of radicals promoting high heat release rate. In deflagration mode, the hydrogen mass is turned towards the wedge wall. In detonation mode, most of the hydrogen is burnt behind the detonation wave, while in deflagration mode some of the unburnt hydrogen is escaped from the domain through the boundary layer. In detonation mode more hydrogen region is exposed towards the incoming air, feeding towards detonation wave, while in deflagration mode lesser hydrogen in exposed towards air. The mass fraction of H_2O is concentrated in front of detonation wave near the wedge wall as well as behind the detonation wave. In deflagration flame mode, the burnt region is bifurcated by H_2 penetration near the wedge wall. The OH mass fraction plot represents the flame front. In detonation mode the flame front is concentrated near the detonation wave, while in deflagration mode, the flame front is lifted and stretched along the wedge. The concentrated detonation wave turns into stretched deflagration flame, with reduced heat release rate as well as reduced maximum pressure in the domain.

It is understood that non-premixed detonation wave configuration is highly unsteady, while in the current discussed case, the unsteady detonation wave remains in the computational domain for most of the time, however there are two incidents of detonation wave turning into deflagration flame and re-establishing itself in detonation mode. Although flow parameters are important to realize detonation wave in non-premixed configuration, the geometric parameters such as wedge angle, angle of injection, distance between the wedge starting and injection points, can play important role in governing the size of shear layer and size of hot burnt gas region near the wall. It may be important to control detonation wave close to the wedge starting point to avoid combustion initiation between shear layer and jet shock to have detonation wave all the time, which can provide high heat release rate as well as higher pressure after the combustion. To control and analyze the non-premixed oblique detonation wave formation for a given flow conditions, the geometric parameters angle of injection and injection location are analyzed in next sections.

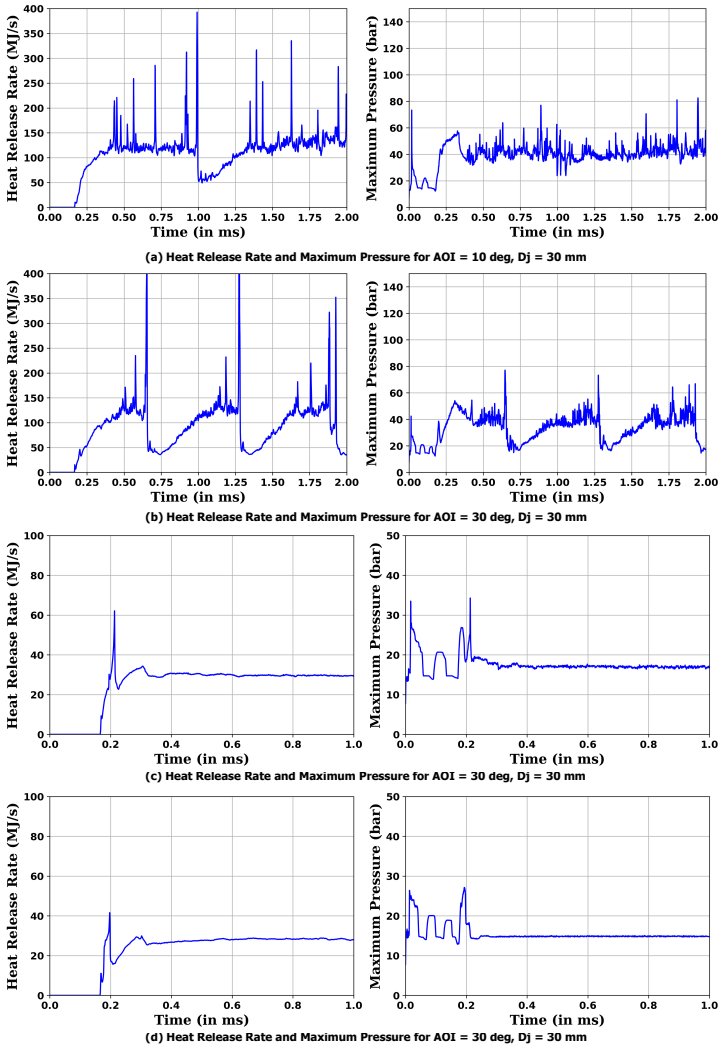

Fig 6. Heat Release Rate and Maximum Pressure for Angle of Injection: AOI = (a) 10°, (b) 30°, (c) 45° and (d) 90° for D_j = 30 mm

3.3. Effect of Angle of Injection

Four additional angles of injection 10°, 30°, 45° and 90° are analyzed along with 15°, while keeping injection location 30 mm from the wedge starting point. The angle of injection 10° and 15° are below the wedge angle of 26°, while 30° is close to the wedge angle. The non-premixed oblique detonation wave pattern consists of jet shock, shear layer and hot burnt gas region. The detonation wave starts near the interaction point of hot burnt gas region and shear layer along with detonation wave. The maximum pressure rise ends after the jet shock interacts with detonation wave. The angle of fuel injection below wedge angle will lead to fuel stream penetration towards the wedge, causing smaller hot burnt gaseous region and situating away from the wedge starting point, which is favourable towards detonation wave formation, avoiding ignition between shear layer and jet-shock. Higher angle of injection may lead to distributed hot burnt gaseous region, prone to ignite fuel-air mixture between larger region of jet-shock and shear layer, causing deflagration mode combustion. Fig 6 a, b, c and d shows the heat release rate and maximum pressure variation for AOI 10°, 30°, 45° and 90°, while keeping injection location same as $D_j = 30$ mm. The heat release rate plot for AOI 10° shows one incident of detonation to deflagration transition around 1 ms, while having detonation mode combustion of higher heat release rate rest of the simulation time. The maximum pressure fluctuates around 40 bar in this case. The heat release rate

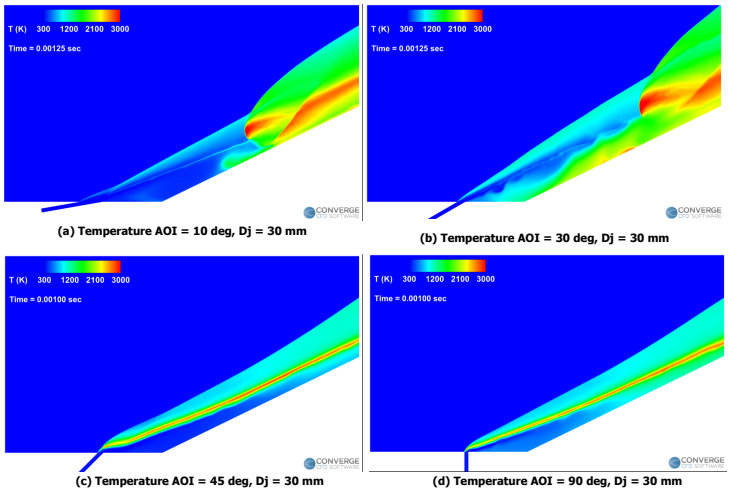

Fig 7. Temperature Contours for Injection: AOI = (a) $10°$, (b) $30°$, (c) $45°$ and (d) $90°$ for D_j = 30 mm

for AOI $30°$ shows more cyclic pattern as it may be considered that the AOI is approximately parallel to wedge angle, leads to higher tendency of detonation to deflagration transition. Further higher AOI $45°$ and $90°$ shows only deflagration mode combustion, leading to lower maximum pressure and lower heat release rate. The deflagration mode combustion is almost steady, once it is established for AOI $45°$ and $90°$.

Figure 7 shows the temperature contours for above four fuel injection angles with injector location 30 mm from wedge tip. The detonation patterns are analyzed with these temperature plots for AOI $10°$ and $30°$. For AOI $10°$, the lifted detonation wave front forms near the wedge starting point with smaller hot burnt zone. The secondary detonation front close to wedge outlet is separated behind the primary lifted detonation front. For AOI $15°$ (in Fig. 4 a), the secondary detonation front is weak and attached to primary lifted detonation wave. For AOI $30°$ slightly higher than the wedge angle, the hot burnt zone is larger and distributed in comparison to AOI $15°$ case. There is a significant larger region between shear layer and jet shock, which is prone to ignition and causes more incidents of detonation to deflagration transition (3 incidents in Fig. 6 b). In case of angle of injection higher than the wedge angle (AOI $45°$ and $90°$), the detonation front is not observed, only stretched deflagration flame is observed, starting from jet bow-shock to the outlet in lifted manner, approximately parallel to wedge. In case of AOI $90°$, the flame thickness is smaller in comparison to AOI $45°$, causes smaller pressure rise. It was also observed that there is lower mass-flow rate for AOI $90°$ case, because of stronger jet bow shock formation at injection point and fuel jet experiences higher pressure at the end of injection tube.

3.4. Effect of Injection Location

Along with variation in AOI, three additional case of variation in injection location as D_j = 10, 50 and 70 mm are also simulated and analyzed along with D_j = 30 mm for AOI $15°$. The heat release rate and maximum pressure observed during the simulation duration are plotted in Fig. 8 for all three cases. Additionally the temperature contours for all three cases are also plotted in Fig. 9. When the fuel is injected near the wedge starting point for D_j = 10 mm, there are cyclic transitions between detonation to deflagration and deflagration to detonation observed for 5 cycles, represented by cycles in heat release rate and maximum pressure. The bifurcated detonation front (primary and secondary) are observed in Fig. 9 a, closer to wedge starting point. The cyclic nature of combustion mode transitions are understood due to impact of shear layer as the hot burnt regions grows and completely dissipated due to high frequency activities of shear layer. In case of D_j = 30 mm, the hot burnt region is formed slightly downstream of wedge in comparison to D_j = 10 mm and larger in size. It may be possible that the larger hot burnt region before detonation wave may absorbs the vortices formed by shear layer and produce damping effect. However, for D_j = 50 mm, the hot burnt region is well distributed from downstream of injector location up to the detonation wave near the end of wedge. The detonation to deflagration

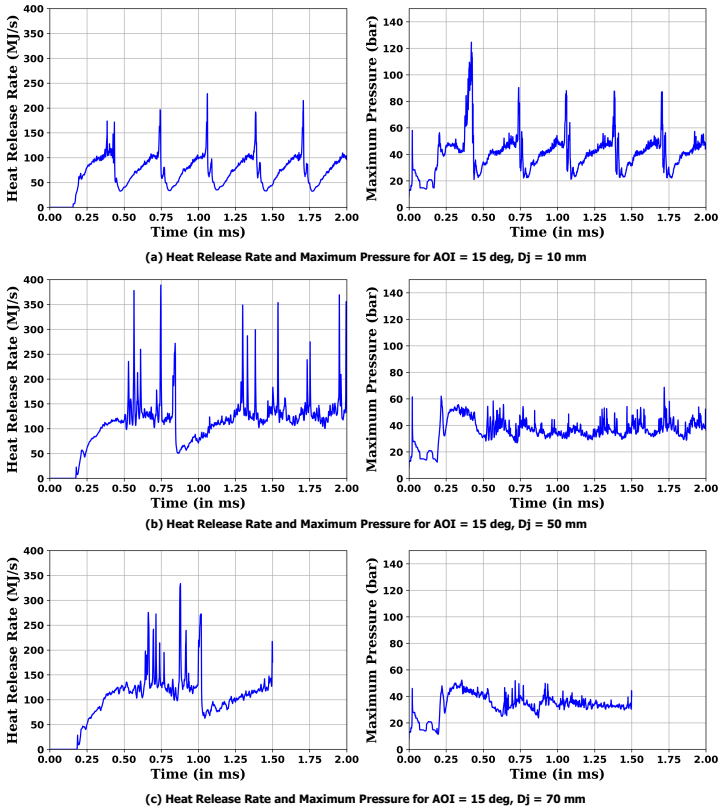

Fig 8. Heat Release Rate and Maximum Pressure for Injection Location at AOI = 15° (a) D_j = 10 mm (b) D_j = 50 mm (c) D_j = 70 mm

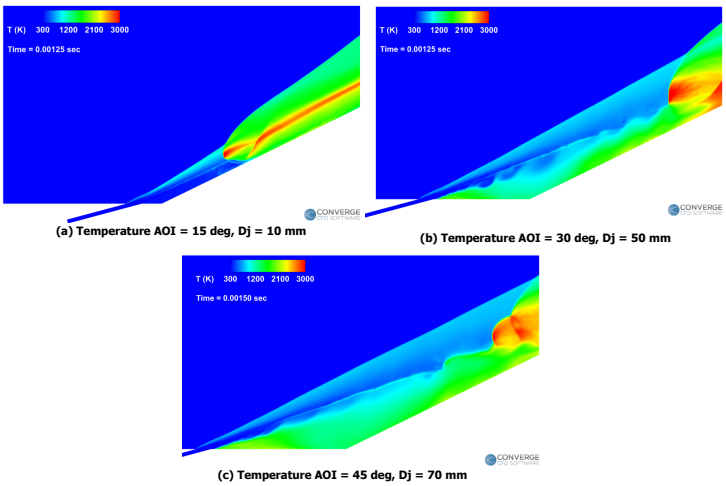

Fig 9. Temperature Contours for for Injection Location at AOI = 15° (a) D_j = 10 mm (b) D_j = 50 mm (c) D_j = 70 mm

transition occurs only once, while many incidents of multi-detonation fronts are observed as reflected in heat release rate and maximum pressure plots in Fig. 8 b. In case of D_j = 70 mm, similar pattern of detonation wave is observed in temperature contours as D_j = 50 mm (Fig. 9b, c). Although the hot burnt region is significantly bigger in size and detonation wave is closer to outlet. The simulation for D_j = 70 mm was stopped at 1.6 ms due to detonation wave placed very closer to the outlet, causes numerical

instability. Hence, the results are plotted (in Fig. 8c) up to 1.5 ms. It can be concluded from the above discussion that increase in distance of injection location fron wedge tip, leads to bigger and distributed hot burnt zone upstream of detonation wave. The detonation wave becomes more stable with increase in injection location, located downstream of wedge, while it depends on multiple detonation initiation to sustain. When the injection location is very close to wedge starting point, the vortex interaction of shear layer dominates the flow field and causes cyclic transition between detonation and deflagration modes, due to smaller hot burnt zone. The larger vortices in shear layer can entrain the mass from hot burnt zone between jet shock and shear layer, causing ignition in the zone and frequent deflagration flame formation than compare to higher distance of injector location cases.

3.5. Thermal and Combustion Efficiency

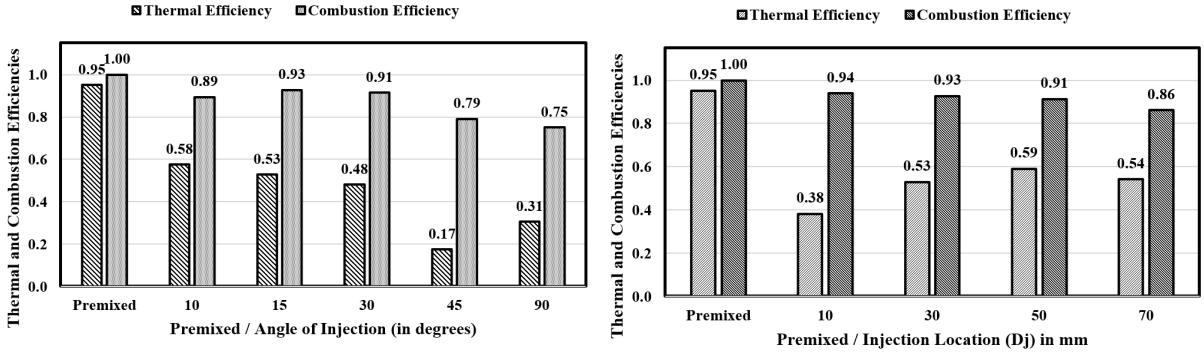

(a) Thermal and Combustion Efficiencies for AOI Variation

(b) Thermal and Combustion Efficiencies for Dj Variation

Fig 10. Thermal and Combustion Efficiencies (a) AOI Variation (b) D_jVariation

The overall performance of studied configuration are compared by computing thermal and combustion efficiencies based on Eq. 1. Figure 10 a and b show the comparison between thermal and combustion efficiencies for AOI variation and injector location variation, respectively. The efficiencies of premixed case are also plotted to provide further understanding. The combustion efficiency is a measure of unburnt H_2 in the domain at the end of simulation time of 2 ms, while thermal efficiency is a measure of total heat release during combustion. The detonation mode combustion has higher heat release rate, while deflagration mode combustion has lower heat release rate. The integrated heat release for a given case (with both detonation and deflagration mode) considers total heat release during the simulation time. If the case shows higher deflagration mode than the detonation mode, the thermal efficiency can be lower. In premixed case there is possibility of small unburnt H_2 escaping along wall boundary, leads to overall thermal efficiency as 0.95, while combustion efficiency is close to 1.0. The premixed detonation case can be assumed ideal case with homogeneous fuel-air mixture. In non-premixed oblique detonation cases with variation in angle of injection (Fig. 10 a, the thermal efficiency decreases with increase in angle of injection, showing highest thermal efficiency for AOI 10° as 0.58. For AOI 15° and 30°, the thermal efficiencies reduced to 0.53 and 0.48, respectively as the increase in AOI causes increase in incidents of detonation to deflagration transitions, leads to overall lower integrated heat release. For AOI 45° and 90°, the deflagration flame configuration, the thermal efficiency reduces to 0.17 and 0.31, respectively. The increase in thermal efficiency for 90° is caused by lower massflow of H_2 into domain, but in both deflagration configuration the thermal efficiencies are far lower than the detonation modes for lower AOI. The unburnt H_2 remaining in the domain is almost same for lower AOI with detonation mode, leads to combustion efficiency as 0.89, 0.93, 0.91 for AOI 10°, 15° and 30°, respectively. For higher AOI 45° and 90° in deflagration mode, the unburnt hydrogen penetrate the boundary layer along the wedge wall and can escape without burning, leads to lower combustion efficiencies as 0.79 and 0.75, respectively.

Fig. 10b shows the thermal and combustion efficiencies for variation in injector locations. The thermal efficiency increases with increase in distance between injection location and wedge tip. For D_j = 10 mm, the thermal efficiency is quite lower as 0.38, due to multi-cycle detonation and deflagration transitions

within the simulation duration, which increases to 0.53 and 0.59 for D_j = 30 mm and 50 mm, respectively due to lower incidents of detonation to deflagration transitions. In case of D_j = 70 mm, the thermal efficiency is slightly reduced to 0.54. The combustion efficiencies are between 0.86 and 0.94 because the oblique detonation modes are exhibited by all the cases.

4. Conclusions

The numerical study of wedge induced oblique detonation wave formation in non-premixed operation of hydrogen injection in hypersonic flow is performed. The flow patterns of unsteady detonation mode combustion and its transition to deflagration flame are observed for a selected angle of injection and location of injector. Further, the impact of angle of injection and injector location on detonation wave formation is analyzed to control the transitions of detonation wave to deflagration flame. Additionally, the thermal and combustion efficiencies are compared for various case. From the obtained results, following are concluded:

1. The operation of non-premixed oblique detonation combustion in scramjet configuration requires efficient fuel injection strategies at before the tip of finite length wedge.

2. The mixing controlled non-premixed oblique detonation wave formation consists of various flow features such as jet-shock, shear layer, hot unburnt region near wedge wall, lifted primary detonation front, wedge wall attached secondary detonation front. The non-premixed oblique detonation wave formation is essentially highly unsteady in nature due to interactions among above flow features. These interactions can lead to momentarily transition of detonation wave to deflagration flame and again re-establishing detonation wave in multiple cycles. The hot burnt zone attached to wedge wall plays important role in these transitions.

3. For the studied flow (Mach = 7, P_∞ = 40 kPa, T_∞ = 300 K, $\theta_w = 30^\circ$) and fuel injection (M_j = 1, $\phi = 0.5$) conditions, the unsteady oblique detonation wave can be observed for fuel injection angles close to or below wedge angle, while for the fuel angle of injection higher than wedge angle only stable deflagration flame is observed. The number of incidents of detonation to deflagration transition increases with increase in angle of injection (AOI) up to 30°.

4. The increase in injector location (for AOI = 15°) from the wedge tip leads to reduce number of cycles of detonation to deflagration transitions. The closer injector location (D_j = 10 mm) near the wedge tip leads detonation front closer to wedge tip and multi-cycle detonation to deflagration transitions, while farther injector locations from the wedge tip leads to detonation front forming downstream on the wedge and lesser transitions to deflagration flames.

5. During the simulation, more number of cycles of detonation to deflagration transitions leads to lower overall thermal efficiency (based on integrated heat release), while lesser incidents leads to higher thermal efficiency. The combustion efficiency (based on unburnt H_2) remains closer for the cases of detonation formation, while reduced only for deflagration mode combustion.

In future studies, the three dimensional nature of fuel injection will be explored along with effects of various flow parameters for mixing controlled non-premixed detonation wave formation.

Acknowledgement

The authors would like to thank Convergent Science for their consistent support and access to CONVERGE solver.

References

[1] Lee, J. H. S., The Detonation Phenomenon. Cambridge University Press (2008).

[2] Wolanski P., Detonative propulsion, Procs. of the Combs. Inst., Vol. 34, no. 1, pp. 125-158, (2013). DOI: 10.1016/j.proci.2012.10.005

[3] Urzay, Javier, "Supersonic Combustion in Air-Breathing Propulsion Systems for Hypersonic Flight", Annual Review of Fluid Mechanics, Vol. 50 pp. 593-627, (2018) DOI:10.1146/annurev-fluid-122316-045217

[4] David W. Bogdanoff D.W., "Advanced injection and mixing techniques for scramjet combustors", Journal of Propulsion and Power, 10:2, 183-190 (1994) DOI:10.2514/3.23728

[5] R. Dudebout R., Sislian J.P., and Oppitz R.,"Numerical Simulation of Hypersonic Shock-Induced Combustion Ramjets", Journal of Propulsion and Power 14:6, 869-879 (1998) DOI:10.2514/2.5368

[6] Wang Y. and Sislian J., "Numerical Investigation of Methane and Air Mixing in a Shcramjet Inlet," AIAA 2008-2533, 15th AIAA International Space Planes and Hypersonic Systems and Technologies Conference (2008). DOI:10.2514/6.2008-2533

[7] Zhang Z., Ma K., Zhang W., Han X., Liu Y., Jiang Z., "Numerical investigation of a Mach 9 oblique detonation engine with fuel pre-injection", Aerospace Science and Technology, Vol.105, 106054 (2020) DOI:10.1016/j.ast.2020.106054.

[8] Wang, B., Ren, Z., "Effects of Fuel Concentration Gradient on Stabilization of Oblique Detonation Waves in Kerosene-Air Mixtures". Flow Turbulence Combust 111, 1059-1077 (2023).DOI:10.1007/s10494-023-00425-2

[9] Deiterding R., Parallel adaptive simulation of multi-dimensional detonation structures. PhD thesis, Brandenburgische Technische Universitat Cottbus, (2003).

[10] Deiterding R., "A parallel adaptive method for simulating shock-induced combustion with detailed chemical kinetics in complex domains". Computers & Structures, 87(11):769□1¤7783, (2009) DOI:10.1016/j.compstruc.2008.11.007

[11] Vashishtha A., Panigrahy S., Campi D., Callaghan D., Nolan C., Deiterding R., "Oblique Detonation Wave Control with O_3 and H_2O_2 Sensitization in Hypersonic Flow" Energies, 15(11):4140 (2020). DOI:10.3390/en15114140

[12] Vashishtha A., Callaghan C. and Nolan C., "Drag Control by Hydrogen Injection in Shocked Stagnation Zone of Blunt Nose", IOP Conference Series: Material Science and Engineering, 1024 012110 (2021)DOI:10.1088/1757-899X/1024/1/012110

[13] Harmon P., Vashishtha A., Callaghan D., Nolan C. and Deiterding R, Study of Direct Gas Injection into stagnation zone of Blunt Nose at Hypersonic Flow, AIAA 2021-3529. AIAA Propulsion and Energy 2021 Forum. (2021) 10.2514/6.2021-3529

[14] Pinaki Pal, Gaurav Kumar, Scott A. Drennan, Brent A. Rankin, and Sibendu Som, "Multidimensional Numerical Simulations of Reacting Flow in a Non-Premixed Rotating Detonation Engine", Vol. 4B: Combustion, Fuels, and Emissions of Turbo Expo: Power for Land, Sea, and Air. ASME, (2019). DOI:10.1115/GT2019-91931

[15] Richards K.J., Senecal P.K., and Pomraning E., Converge 3.1. Convergent Science, (2023). https://convergecfd.com/

[16] Kore R., Vashishtha A., "Numerical study of oblique detonation wave control for fuel blends", in proceedings of 57th 3AF International Conference on Applied Aerodynamics (2023) URL: handle/20.500.12065/4538

[17] Westbrook C.K., "Chemical kinetics of hydrocarbon oxidation in gaseous detonations", Combustion and Flame, Vol. 46, pp. 191-210, (1982). DOI: 10.1016/0010-2180(82)90015-3

[18] Palateerdham S.K., Peri L.N.P., Ingenito A., Vashishtha A., "Numerical investigation of the impact of injectors location on fuel mixing in the HIFiRE 2 Scramjet combustor" in proceedings of

Aerospace Europe Conference 2023 - 10th European Conference for Aerospace Sciences (EUCASS) and the 9th conference of the Council of European Aerospace Societies (CEAS) (2024) DOI:10.13009/eucass2023-866